

# Integrated Stress Response Inhibitor Reverses Sex-Dependent Behavioral and Cell-Specific Deficits after Mild Repetitive Head Trauma

Karen Krukowski,<sup>1,2,\*</sup> Amber Nolan,<sup>1–3,\*</sup> Elma S. Frias,<sup>1,2,4</sup> Katherine Grue,<sup>1,2</sup> McKenna Becker,<sup>1,2</sup> Gonzalo Ureta,<sup>5</sup> Luz Delgado,<sup>5</sup> Sebastian Bernales,<sup>5</sup> Vikaas S. Sohal,<sup>6</sup> Peter Walter,<sup>7,8</sup> and Susanna Rosi<sup>1,2,9–11</sup>

## Abstract

Mild repetitive traumatic brain injury (rTBI) induces chronic behavioral and cognitive alterations and increases the risk for dementia. Currently, there are no therapeutic strategies to prevent or mitigate chronic deficits associated with rTBI. Previously we developed an animal model of rTBI that recapitulates the cognitive and behavioral deficits observed in humans. We now report that rTBI results in an increase in risk-taking behavior in male but not female mice. This behavioral phenotype is associated with chronic activation of the integrated stress response and cell-specific synaptic alterations in the type A subtype of layer V pyramidal neurons in the medial prefrontal cortex. Strikingly, by briefly treating animals weeks after injury with ISRIB, a selective inhibitor of the integrated stress response (ISR), we (1) relieve ISR activation, (2) reverse the increased risk-taking behavioral phenotype and maintain this reversal, and (3) restore cell-specific synaptic function in the affected mice. Our results indicate that targeting the ISR even at late time points after injury can permanently reverse behavioral changes. As such, pharmacological inhibition of the ISR emerges as a promising avenue to combat rTBI-induced behavioral dysfunction.

**Keywords:** integrated stress response; prefrontal cortex; repetitive mild traumatic brain injury; risk-taking behavior; synaptic function

## Introduction

**T**RAUMATIC BRAIN INJURY (TBI) is a growing health problem. Approximately five million Americans are living with a TBI related disability,<sup>1–4</sup> and even mild TBI can elicit chronic cognitive dysfunction and functional limitation.<sup>2,3,5</sup> Further, a previous TBI increases the risk for additional TBI,<sup>6–8</sup> making it imperative to understand the potential compounding effects of repetitive trauma. Rising concern for repetitive head trauma has led to an increase in studies of concussive and subconcussive injuries (reviewed in<sup>9,10</sup>). While there is still debate as to the severity of symptoms, the majority of studies report poorer cognitive and behavioral outcomes in individuals after multiple mild head traumas.<sup>9–11</sup> Specifically, increased risk-taking behavior and disinhibited symptoms are often reported by individuals who have had mild single or repetitive traumatic brain injury (rTBI).<sup>12–17</sup> Despite the increased interest in understanding the long-term consequences of rTBI, little is known about the underlying cellular and functional correlates responsible for these maladaptive behavioral and cognitive

changes. With no identified mechanisms, there are no pharmacological treatment options for individuals with rTBI-induced deficits.

The integrated stress response (ISR) is a universal cellular pathway that serves to cope with different cellular stressors,<sup>18</sup> and it is induced after a single TBI.<sup>19–21</sup> In mammals, activation of the ISR modulates protein translation through the phosphorylation of a single serine on the  $\alpha$  subunit of the translation initiation factor eIF2, which leads to a reduction in global protein translation.<sup>22,23</sup> A select number of proteins are up-regulated with ISR activation including the  $\beta$ -site APP-cleaving enzyme 1 (BACE1)<sup>24–27</sup> and activating transcription factor 4 (ATF4).<sup>28,29</sup> Chronic ISR activation creates maladaptive cellular and functional changes including cognitive decline.<sup>19,30–32</sup>

It is not known whether mild rTBI induces ISR activation and whether it plays a role in behavioral changes and the associated neuronal dysfunction in the prefrontal cortex. Recently, we discovered a potent non-toxic ISR inhibitor (ISRIB)<sup>33–35</sup> that reverses cognitive deficits resulting from single impact TBI. When administered weeks after injury, ISRIB treatment reversed memory

Department of <sup>1</sup>Physical Therapy and Rehabilitation Science, <sup>2</sup>Brain and Spinal Injury Center, Departments of <sup>3</sup>Pathology, <sup>4</sup>Biomedical Sciences, <sup>6</sup>Psychiatry, <sup>7</sup>Biochemistry and Biophysics, <sup>8</sup>Howard Hughes Medical Institute, <sup>9</sup>Department of Neurological Surgery, <sup>10</sup>Weill Institute for Neuroscience, <sup>11</sup>Kavli Institute of Fundamental Neuroscience, University of California, San Francisco, California, USA.

<sup>5</sup>Fundación Ciencia & Vida, Santiago, Chile.

\*Contributed equally to first authorship.

deficits in two distinct focal and diffuse TBI rodent models<sup>19</sup> Further, ISRIB reversed trauma-induced suppression in hippocampal long-term potentiation. These findings lay the foundation for targeting the ISR for reversal of trauma-induced behavioral changes in the prefrontal cortex.

Recently we developed a pre-clinical rodent model to investigate cognitive and behavioral outcomes associated with rTBI.<sup>36</sup> In this model, animals receive a mild impact to the head daily for five days. When we investigated behavioral (risk-taking and social behaviors) and cognitive performance (episodic and working memory), we found behavioral impairments in animals that received five mild impacts. This is in line with other studies of rTBI in rodent models<sup>38,39</sup> and corresponds with patient reported outcomes after rTBI.<sup>12–15</sup> Our previous studies did not measure significant changes in the intrinsic excitability of layer V (L5) pyramidal neurons in the medial prefrontal cortex (mPFC), a brain region vital for integration of these complex behaviors.<sup>41,43</sup>

In the current study, we evaluate excitatory synaptic input in L5 pyramidal neurons and explicitly assess function by neuronal subtype, because divergent patterns of synaptic input have been reported in L5 pyramidal neuron subtypes.<sup>41</sup> Specifically, we analyze the two subtypes of L5 pyramidal neurons that project subcortically (“type A”) or callosally to other cortical locations (“type B”).<sup>41</sup> Finally, we investigate whether ISR activation plays a role in these deficits and whether ISRIB treatment can reverse behavioral and cellular changes associated with rTBI.

## Methods

### Animals

All experiments were conducted in accordance with National Institutes of Health (NIH) Guide for the Care and Use of Laboratory Animals and approved by the Institutional Animal Care and Use Committee of the University of California, San Francisco (AN170302). Male and female C57B6/J wild-type mice were received from Jackson Laboratories. Male animals were 8–10 weeks of age at the time of surgeries. Female animals were 10 weeks of age at the time of surgery to ensure full sexual maturity. Animal shipments were received at least one week before the start of experimentation to allow animals to habituate to the new surroundings. Mice were group housed in environmentally controlled conditions with a reverse light cycle (12:12 h light: dark cycle at 21 ± 1°C; ~50% humidity) and provided food and water *ad libitum*.

### Surgical procedure

All animals were assigned randomly to either TBI or sham surgery groups. Animals were anesthetized and maintained at 2–2.5% isoflurane.

### Sham with sutures

Sham with sutures was performed as previously described<sup>37</sup>. Briefly, animals were secured to a stereotaxic frame with non-traumatic ear bars. A midline incision was made to expose the skull and the scalp was sutured.

### Sham with no sutures

Sham without sutures was performed as described previously.<sup>36</sup>

### Repetitive mild TBI

The rTBI animals underwent multiple mild closed head injuries using the CHIMERA (Closed-Head Impact Model of Engineered Rotational Acceleration) device as reported previously.<sup>36,38,39</sup> Briefly, mice were placed supine into an angled holding platform to

ensure the head was level with the piston target hole and that the impact was centered at the midline dorsal convexity of the skull, targeting bregma. A nose cone delivering isoflurane was removed just before impact. The impact was administered with a velocity range of ~3.9–4.5 m/sec, resulting in an impact energy of 0.5 J from the 5 mm, 50 g piston. The rTBI animals received an injury once per day for five days with ~24 h interval in between impacts.

### Focal TBI

Controlled cortical impact (CCI) surgery was performed as described previously.<sup>19,37,40</sup> Briefly, animals were secured to a stereotaxic frame with non-traumatic ear bars. A midline incision was made to expose the skull followed by a ~3.5-mm diameter craniectomy, a removal of part of the skull, using an electric micro-drill. The coordinates of the craniectomy were: anteroposterior, –2.00 mm and mediolateral, +2.00 mm with respect to bregma. Any animal that experienced excessive bleeding because of disruption of the dura was removed from the study.

After the craniectomy, the contusion was induced using a 3-mm convex tip attached to an electromagnetic impactor (Leica). The contusion depth was set to 0.95 mm from dura with a velocity of 4.0 m/sec sustained for 300 msec. After impact, the scalp was sutured. These injury parameters were chosen to target, but not penetrate, the hippocampus.

### Concussive TBI

Closed head injury (CHI) surgery was performed as described previously.<sup>19</sup> Briefly, animals were secured to a stereotaxic frame with non-traumatic ear bars, and the head of the animal was supported with foam before injury. Contusion was induced using a 5-mm convex tip attached to an electromagnetic impactor (Leica) at the following coordinates: anteroposterior, –1.50 mm and mediolateral, 0 mm with respect to bregma. The contusion was produced with an impact depth of 1 mm from the surface of the skull with a velocity of 5.0 m/sec sustained for 300 msec. Any animals that had a fractured skull after injury were excluded from the study. After impact, the scalp was sutured.

The approximate isoflurane exposure for each procedure is as follows: ~20–25 min for CCI and CHI, ~15–25 min for rTBI (3–5 min per exposure and five exposures total), ~20 min for sham with sutures, ~15–25 min for sham without sutures (3–5 min per exposure and five exposures total). After all surgeries, the animal recovered in an incubation chamber set to 37°C. Animals were returned to their home cage after showing normal walking and grooming behavior. All animals fully recovered from the surgical procedures as exhibited by normal behavior and weight maintenance monitored throughout the duration of the experiments.

### Drug administration

The ISRIB solution was made by dissolving 5 mg ISRIB in 1 mL dimethyl sulfoxide (DMSO) (PanReac AppliChem, 191954.1611). The solution was heated gently in a 40°C water bath and vortexed every 30 sec until the solution became clear. Next, 1 mL of Tween 80 (Sigma Aldrich, P8074) was added, solution was heated gently in a 40°C water bath and vortexed every 30 sec until the solution became clear. Next, 10 mL of polyethylene glycol 400 (PEG400) (PanReac AppliChem, 142436.1611) solution was added, heated gently in a 40°C water bath and vortexed every 30 sec until the solution became clear. Finally, 36.5 mL of 5% dextrose (Hospira, RL-3040) was added. The solution was kept at room temperature throughout the experiment. Each solution was used for injections up to 7 days maximum. The vehicle solution consisted of the same chemical composition and concentration (DMSO, Tween 80, PEG400, and 5% dextrose).

Stock ISRIB solution was at 0.1 mg/mL, but injections were at 2.5 mg/kg. We reported previously that a dose of 2.5 mg/kg

reversed trauma-induced cognitive decline<sup>19</sup> and improved memory function in healthy animals.<sup>33</sup> In addition, we identified that a minimal dosing paradigm (3–4 treatments) was sufficient for learning and memory rescue.<sup>19</sup>

### Risk-taking behavioral test

For all behavioral assays, the experimenters were blinded to surgery and drug intervention. Before behavioral analysis, animals were inspected for gross motor impairments. Animals were inspected for suture healing, whisker loss, limb immobility (including grip strength), and eye occlusions. If animals displayed *any* of these impairments, they were eliminated from the study. Behavioral tests were recorded and scored using a video tracking and analysis setup (Ethovision XT 8.5, Noldus Information Technology). If tracking was unsuccessful, videos were scored by two individuals blinded to surgery and treatment group.

Risk-taking behavioral phenotype was evaluated using the Elevated Plus Maze (EPM) between 21–31 days (~one month) post-injury (counted from the day of the first injury) as described previously.<sup>36</sup> The EPM consists of two exposed, open arms (35 cm) opposite each other and two enclosed arms (30.5 cm) also across from each other. The four arms are attached to a center platform (4.5 cm square), and the entire maze is elevated 40 cm off the floor. Bright white lights illuminated both ends of the open arm. Mice were placed individually onto the center of the maze and allowed to explore the maze for 5 min, and their activity was recorded. The maze was cleaned with 70% ethanol between animals. Risk-taking behavior was measured by changes in time spent in the open arms + center.

No difference in time spent exploring the open arms was observed when comparing the sham animals ± sutures and animals ± vehicle injections (Supplementary Table 1); therefore, sham groups were combined for analysis. No differences in time spent exploring the open arms were observed when comparing the rTBI ± vehicle injections (Supplementary Table 2); thus, rTBI groups were combined for analysis. Finally, no differences were observed when comparing animals that were exposed to the EPM once or twice (with three months in between exposures, Supplementary Table 3).

### Western blot analysis

At the end of the behavioral test, animals were sacrificed, and the hemibrains were extracted and snap frozen on dry ice and then stored at  $-80^{\circ}\text{C}$ . Hemibrains were used for protein analysis because preliminary analysis found insufficient protein amounts (ATF4, BACE-1) in isolated brain regions. The frozen samples were then homogenized with a T 10 basic ULTRA-TURRAX (IKA) in ice-cold buffer lysis (Cell Signaling 9803) and protease and phosphatase inhibitors (Roche). Lysates were sonicated for 3 min and centrifuged at 13,000 rpm for 20 min at  $4^{\circ}\text{C}$ .

Protein concentration in supernatants was determined using BCA Protein Assay Kit (Pierce). Equal amount of proteins (30  $\mu\text{g}$ ) was loaded on SDS-PAGE gels. Proteins were transferred onto 0.2  $\mu\text{m}$  PVDF membranes (BioRad) and probed with primary antibodies diluted in Tris-buffered saline supplemented with 0.1% Tween 20 and 3% bovine serum albumin.

Phospho-eIF2 $\alpha$  (Cell Signaling), eIF2 $\alpha$  (Cell Signaling, Danvers, MA), BACE-1 (Cell Signaling), ATF4 (Abcam), and  $\beta$ -actin (Sigma-Aldrich) antibodies were used as primary antibodies. The horseradish peroxidase (HRP)-conjugated secondary antibodies (Rockland) were employed to detect immune-reactive bands using enhanced chemiluminescence (ECL Western Blotting Substrate, Pierce) according to the manufacturer's instructions. Quantification of protein bands was performed by densitometry using ImageJ software.

Phospho-eIF2 $\alpha$  was normalized to total eIF2 protein levels. The ATF4 and BACE-1 levels were normalized to  $\beta$ -actin expression,

and fold change is calculated as the levels relative to the expression in sham + vehicle-treated derived samples.

### Electrophysiology

Coronal brain slices (250  $\mu\text{m}$ ) including the mPFC were prepared from mice that underwent rTBI or a sham procedure, 35–60 days prior, as well as mice that underwent rTBI and received an ISRIB injection at ~30 days post-injury. To conserve mice, a sham group that received an ISRIB injection was not included, because there was no difference in EPM behavior at 1 month after injury between sham mice alone compared with sham + ISRIB mice.

Mice were anesthetized with Euthasol (0.1 mL/25 g, Virbac, Fort Worth, TX, NDC-051311-050-01), and transcardially perfused with an ice-cold sucrose solution containing (in mM): 210 sucrose, 1.25  $\text{NaH}_2\text{PO}_4$ , 25  $\text{NaHCO}_3$ , 2.5 KCl, 0.5  $\text{CaCl}_2$ , 7  $\text{MgCl}_2$ , 7 dextrose, 1.3 ascorbic acid, 3 sodium pyruvate (bubbled with 95%  $\text{O}_2$ –5%  $\text{CO}_2$ , pH ~7.4) (see Supplementary Table 4 for reagent information). Mice were then decapitated, and the brain was isolated in the same sucrose solution and cut on a slicing vibratome (Leica, VT1200S, Leica Microsystems, Wetzlar, Germany). Slices were incubated in a holding solution (composed of (in mM) 125 NaCl, 2.5 KCl, 1.25  $\text{NaH}_2\text{PO}_4$ , 25  $\text{NaHCO}_3$ , 2  $\text{CaCl}_2$ , 2  $\text{MgCl}_2$ , 10 dextrose, 1.3 ascorbic acid, 3 sodium pyruvate, bubbled with 95%  $\text{O}_2$ –5%  $\text{CO}_2$ , pH ~7.4) at  $36^{\circ}\text{C}$  for 30 min and then at room temperature for at least 30 min until recording.

Whole cell recordings were obtained from these slices in a submersion chamber with a heated ( $32$ – $34^{\circ}\text{C}$ ) artificial cerebrospinal fluid (aCSF) containing (in mM): 125 NaCl, 3 KCl, 1.25  $\text{NaH}_2\text{PO}_4$ , 25  $\text{NaHCO}_3$ , 2  $\text{CaCl}_2$ , 1  $\text{MgCl}_2$ , 10 dextrose (bubbled with 95%  $\text{O}_2$ /5%  $\text{CO}_2$ , pH ~7.4). Patch pipettes (3–6  $\text{M}\Omega$ ) were manufactured from filamented borosilicate glass capillaries (Sutter Instruments, Novato, CA, BF100-58-10) and filled with an intracellular solution containing (in mM): 135 Kgluconate, 5 KCl, 10 HEPES, 4 NaCl, 4  $\text{MgATP}$ , 0.3  $\text{Na}_3\text{GTP}$ , 7 2K-phosphocreatine, and 1–2% biocytin. Layer V pyramidal neurons were identified using infrared microscopy with a 40 $\times$  water-immersion objective (Olympus, Burlingame, CA).

Recordings were made using a Multiclamp 700B (Molecular Devices, San Jose, CA) amplifier, which was connected to the computer with a Digidata 1440A ADC (Molecular Devices, San Jose, CA), and recorded at a sampling rate of 20 kHz with pClamp software (Molecular Devices). We did not correct for the junction potential, but access resistance and pipette capacitance were appropriately compensated before each recording.

The passive membrane and active action potential (AP) spiking characteristics were assessed by injection of a series of hyperpolarizing and depolarizing current steps with a duration of 250 msec from  $-250$  pA to 700 pA (in increments of 50 pA). The resting membrane potential was the measured voltage of the cell 5 min after obtaining whole cell configuration without current injection; this value thus represents the resting potential of the cell after internal dialysis with the intracellular solution reported above. A holding current was then applied to maintain the neuron at  $-67$  mV before/after current injections. The membrane resistance was determined from the steady-state voltage reached during the  $-50$  pA current injection. The time constant was the time required to reach 63% of the maximum change in voltage for the  $-50$  pA current injection.

The AP parameters including the half width, threshold, amplitude, and spike afterhyperpolarization (AHP) were measured from the current injection that was 100 pA above the first current injection that elicited spiking. The AP times were detected by recording the time at which the positive slope of the membrane potential crossed 0 mV. From the AP times, the instantaneous frequency for each AP was determined (1/inter spike interval). The AP rate as a function of current injection was examined by plotting the first instantaneous AP frequency versus current injection

amplitude. The F/I slope was then determined from the best linear fit of the positive values of this plot.

The AP or spike threshold was defined as the voltage at which the third derivative of  $V$  ( $d^3V/dt$ ) was maximal just before the AP peak. The AP amplitude was calculated by measuring the voltage difference between the peak voltage of the AP and the spike threshold. The half width of the AP was determined as the duration of the AP at half the amplitude. The spike AHP was the voltage difference between the AP threshold and the minimum voltage before the next AP. The rising and falling slopes of the AP were the maximum of the first derivative of  $V$  between the threshold to the peak amplitude, and the peak amplitude to the minimum voltage before the next AP, respectively. The adaptation index of each cell was the ratio of the last over the first instantaneous firing frequency, calculated at 250 pA above the current step that first elicited spiking.

Subthreshold properties indicative of the degree of  $I_H$  current were assessed with two parameters: (1) the voltage sag—defined as the change in voltage between the maximum hyperpolarization and the steady state potential for the  $-200$  pA current injection; (2) the rebound afterdepolarization (ADP)—defined as the change in voltage between the maximum depolarization and the steady state potential achieved immediately after ending the  $-200$  pA current injection. Finally, the rebound AHP was measured as the change in voltage between the maximum hyperpolarization and the steady state potential achieved immediately after ending the  $+250$  pA current injection. The sum of these three variables was used as described previously to categorize pyramidal neurons as type A ( $> 6.5$  mV) or type B ( $< 6.5$  mV)<sup>41</sup>.

To measure the spontaneous excitatory post-synaptic currents (sEPSCs), cells were recorded in voltage clamp at a holding potential of  $-75$  mV for 4 min, a holding potential that should have little inhibitory component given the reversal potential of chloride with these solutions. Analysis of sEPSCs was performed using a template matching algorithm in ClampFit 10.7 (Molecular Devices, San Jose, CA). The template was created using recordings from multiple pyramidal cells and included several hundred synaptic events.

Access resistance ( $R_a$ ) was monitored during recordings, and recordings were terminated if  $R_a$  exceeded 30 megaohms. Only stable recordings ( $< 50$  pA baseline change) with a low baseline noise ( $< 8$  pA root mean square) were included. The first 250 synaptic events or all the events measured in the 4 min interval from each cell were included for analysis. The median frequency and amplitude for these events was calculated for each cell to compare between groups.

### Statistical analysis

All data were analyzed with GraphPad Prism 8 statistical software. Statistical significance between groups for most variables was determined using a two-tailed  $t$  test, one-way analysis of variance (ANOVA), or two-way ANOVA. If data were outside of the normal distribution as indicated by an alpha  $< 0.01$  for both D'Agostino-Pearson omnibus and Shapiro-Wilk tests, a non-parametric test was used—specifically, a Kruskal-Wallis test was used for the electrophysiology parameters. The firing responses to increasing current injections were analyzed as a repeated measures two-way ANOVA. The  $p$  values below 0.05 were considered significant.

## Results

### Repetitive mild TBI increases risk-taking behaviors in male but not female cohorts

We reported previously that five mild rTBI resulted in increased risk-taking behaviors in male rodents.<sup>36</sup> Here we wanted to deter-

mine whether the changes in risk-taking behavior measured after rTBI are also observed after other commonly used single injury models and whether female mice are impaired equally. We compared trauma-induced behavioral deficits between: (1) five rTBIs,<sup>36</sup> (2) a single mild concussive closed head injury (CHI),<sup>19</sup> (3) a moderate, focal injury model—CCI,<sup>19,37,40</sup> and (4) sham surgery in male and female mice.

We evaluated changes in risk-taking behavior approximately one-month post-injury with the EPM testing paradigm (Fig. 1A). In the EPM, animals are positioned in the center of a four-arm arena and allowed to freely explore the maze composed of two dark arms and two brightly illuminated arms for 5 min. Healthy rodents explore all the arms but spend the majority of time in the closed arms.<sup>42</sup> Increased time spent exploring the open arms denotes increased risk-taking behavior. When comparing different trauma models, we found that only male mice that received rTBI spent significantly more time in the open arms compared with sham control animals (Fig. 1B).

None of the injury models evaluated impacted risk-taking behavior in the female cohorts (Fig. 1C). When comparing male and female rTBI mice, we measured a significant sex-dependent injury effect; further, we did not observe differences in the time spent in the open arms when comparing male and female sham animals. These results demonstrate that rTBI results in increased risk-taking behavior in male but not in female mice. Because no deficits were observed in female mice, we focused on rTBI-induced cellular changes in male mice.

### ISR is activated at one month after rTBI

Aberrant activation of the ISR has been measured acutely and chronically in different models of TBI.<sup>19–21</sup> We investigated whether mild rTBI induces chronic activation of the ISR by quantifying p-eIF2 $\alpha$ , ATF4, and BACE-1 levels in hemibrain lysates  $\sim$ one month post-injury (Supplementary Fig. 1). When investigating the impact of rTBI and ISRIB on p-eIF2 $\alpha$  protein expression, we measured a significant injury ( $p < 0.001$ ) and ISRIB effect ( $p < 0.01$ ) (Fig. 2A). Downstream modulators of ISR activation, ATF4 and BACE-1, were significantly increased when comparing sham and rTBI male mice (Fig. 2B,C). Importantly, ISRIB administration reversed rTBI-induced ISR activation and downstream modulators to levels comparable to sham animals (Fig. 2). These data indicate that rTBI triggers a persistent activation of the ISR and that ISRIB can relieve this activation.

### ISRIB reverses rTBI-mediated increased risk-taking behavior

We demonstrated previously that ISR inhibition with the small molecule ISRIB can fully reverse trauma-induced hippocampal-dependent learning and memory deficits.<sup>19</sup> Here, we investigated whether ISR inhibition can reverse the increased risk-taking behavior. Male mice received five mild head injuries or sham surgery. We then assessed risk-taking behavior one month post-injury with the EPM (Fig. 3A). The evening before EPM (day 30), animals received intraperitoneal injections of ISRIB (2.5 mg/kg) or vehicle (Fig. 3A). Quantification of the time spent in the open arms was indistinguishable when comparing rTBI + ISRIB and sham groups (Fig. 3B). Notably, a single injection of ISRIB was sufficient to reverse the rTBI-induced risk-taking phenotype.

Next, we investigated whether ISRIB could permanently reverse rTBI-induced risk-taking behavior. Animals received two additional doses of ISRIB, one immediately after EPM (day 31) and one

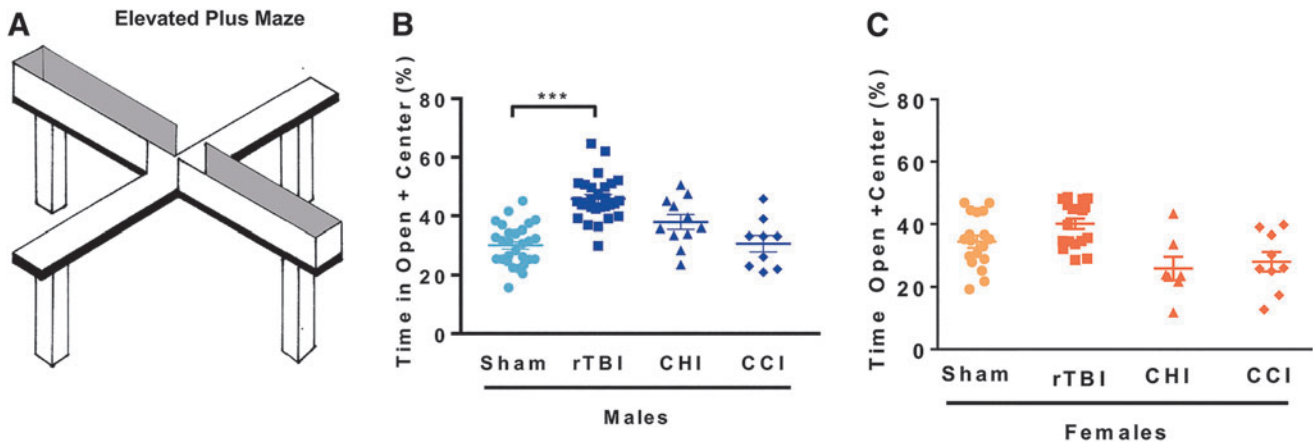


**FIG. 1.** Repetitive mild traumatic brain injury (rTBI) increases risk-taking behaviors in male but not female cohorts. Risk-taking behavior was measured in the elevated plus maze by increased time spent in the open arms (including center space). Comparison of three rodent trauma models found that risk-taking behavior was only measured after mild repetitive trauma in male cohorts. (A) Schematic of the elevated plus maze. (B) Male mice were exposed to either (1) mild rTBI, (2) mild concussive injury-closed head injury (CHI), (3) moderate focal injury-controlled cortical impact (CCI), or (4) sham surgery; risk-taking behavior was measured 30 days post-injury. Significant increases in time spent in the open arm were measured after rTBI. (C) Female mice were exposed to either (1) rTBI, (2) CHI, (3) CCI, or (4) sham surgery; risk-taking behavior was measured one month post-injury. No differences in risk-taking behavior were measured between groups. Two-way analysis of variance measured significant injury ( $p < 0.001$ ), sex effects ( $p < 0.001$ ), and interaction ( $p < 0.001$ ). Tukey *post hoc* analysis revealed group differences. Individual animal scores represented in dots; lines depict group mean and standard error of the mean. Color image is available online.

the next day (day 32, Fig. 3A—three doses in total<sup>19</sup>). At ~three months (100 days) post-injury, we measured risk-taking behavior. No additional doses of ISRIB were administered after the initial three injections (Fig. 3A). Once again, rTBI + vehicle animals displayed significant increases in time spent in the open arms of the EPM (Fig. 3C). Importantly, the three ISRIB injections administered ~70 days prior reversed long-term rTBI-induced risk-taking behavior (Fig. 3C). The ISRIB administration also reduced time spent in the open arms in sham animals. These data demonstrate that a pulse administration of ISRIB, one month after injury, can completely reverse the long-lasting risk-taking behavior phenotype after rTBI.

#### ISRIB treatment restores cell-specific vulnerability in type A layer V pyramidal neurons of the mPFC after rTBI

The mPFC is a brain region implicated in complex behaviors, including contextual response and risk-taking behavior.<sup>43</sup> To investigate the neurophysiological correlates of risk-taking behavior after rTBI and ISRIB treatment, we evaluated the intrinsic and synaptic properties of layer V pyramidal neurons in the mPFC, the primary output of the microcircuit. Layer V pyramidal neurons include at least two subtypes, denoted type A and type B, characterized by their morphology, intrinsic ion channel composition, and

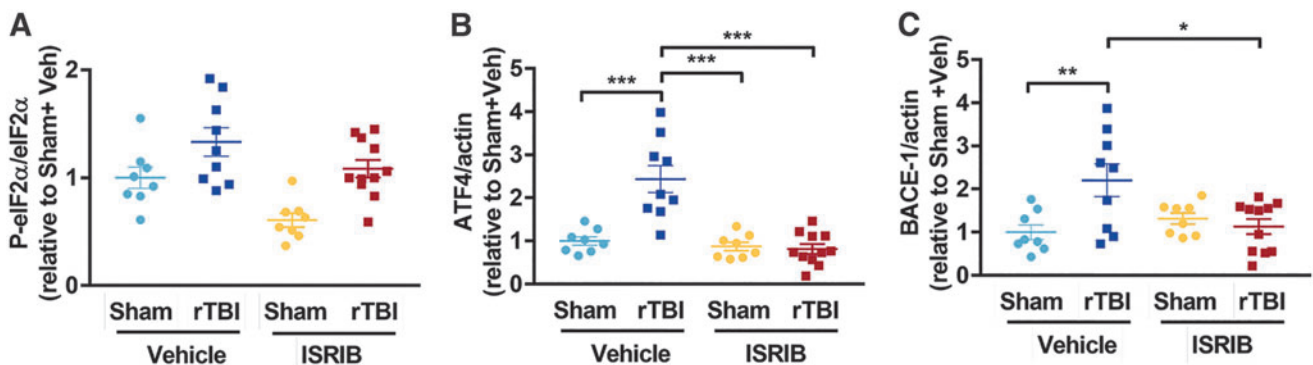


**FIG. 2.** Integrated stress response (ISR) activation one month after repetitive mild traumatic brain injury (rTBI). The impact of rTBI on ISR activation was investigated by Western blot analysis of hemibrain lysates. (A) Mild rTBI induced increases in p-eIF2 $\alpha$  protein levels one month post-injury. The p-eIF2 $\alpha$  protein levels normalized to total eIF2 $\alpha$  and standardized to sham vehicle group. Two-way analysis of variance (ANOVA) revealed a significant injury ( $p < 0.001$ ), and ISR inhibitor (ISRIB) effect ( $p < 0.01$ ). The rTBI significantly increased (B) ATF4 and (C) BACE-1 protein levels. The ISRIB treatment reversed rTBI-induced increases. (B) Two-way ANOVA revealed a significant injury ( $p < 0.001$ ), ISRIB ( $p < 0.001$ ) and ISRIB  $\times$  injury effect ( $p < 0.001$ ). Tukey *post hoc* analysis revealed differences between groups. (C) Two-way ANOVA revealed a significant injury ( $p < 0.05$ ) and ISRIB  $\times$  injury effect ( $p < 0.01$ ). Tukey *post hoc* analysis revealed differences between groups. Individual animal scores represented in dots; lines depict group mean and standard error of the mean. Color image is available online.

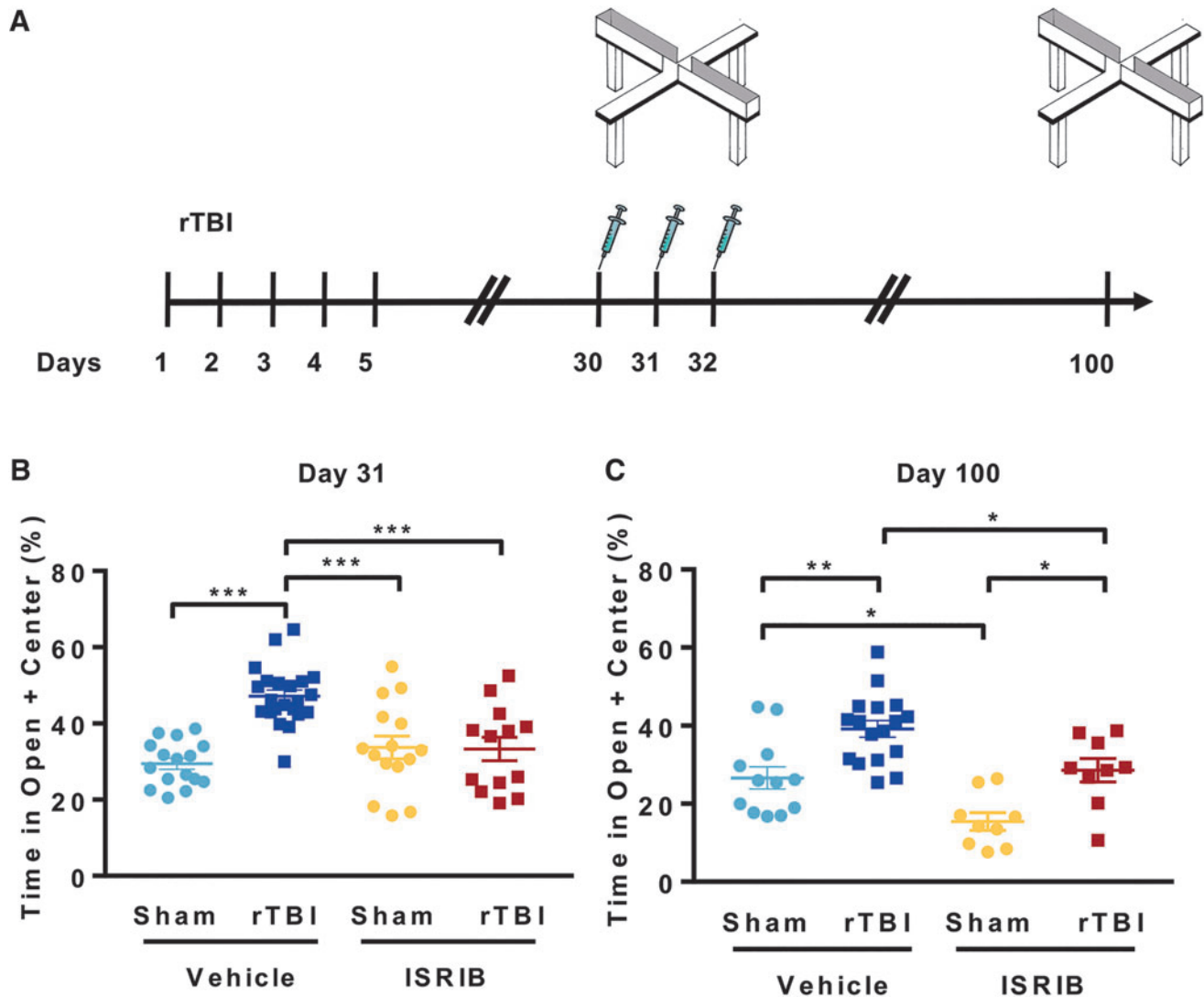


**FIG. 3.** Small molecule integrated stress response inhibitor, ISRIB, reverses repetitive traumatic brain injury (rTBI) mediated risk-taking behavior. (A) Experimental Design. Elevated Plus maze was performed at ~31 and 100 days post-injury (dpi). The ISRIB (2.5 mg/kg intraperitoneal) was administered on days 30, 31, and 32 dpi. (B) A single ISRIB dose (2.5 mg/kg intraperitoneal) reversed trauma-induced risk-taking behavior at one month post-surgery. Two-way analysis of variance (ANOVA) measures significant injury ( $p < 0.001$ ), ISRIB ( $p < 0.05$ ), and ISRIB  $\times$  injury effect ( $p < 0.001$ ). Tukey *post hoc* analysis revealed differences between groups. (C) Permanent changes in risk-taking behavior were observed at ~3 months (100 days) post-injury. Three injections of ISRIB (70 days prior) completely reversed trauma-induced behavioral changes. Two-way ANOVA measures significant injury ( $p < 0.001$ ) and ISRIB ( $p < 0.001$ ) effect. Tukey *post hoc* analysis revealed differences between groups. Individual animal scores represented in dots; lines depict group mean and standard error of the mean. Color image is available online.

axonal projections to primarily subcortical or other cortical regions, respectively<sup>41</sup> (Fig. 4A, 5A).

We distinguished these layer V neuronal subtypes by their electrophysiological properties (with prominence of the  $I_h$ -induced parameters in type A neurons including the sag and rebound in response to hyperpolarization, as well as the afterhyperpolarization after depolarization), as reported previously.<sup>41</sup> We detected no effect of trauma on the intrinsic excitability of either type A or type B neurons, similar to our previous results that grouped layer V neurons together<sup>36</sup> (Supplementary Fig. 2 and 3, Supplementary Tables 5 and 6).

Conversely, we found a cell-specific change in synaptic input after rTBI. Specifically, type A neurons demonstrated a significant increase in the frequency of spontaneous excitatory synaptic cur-

rents (sEPSC) after rTBI (Fig. 4B,C) without changes in the amplitude of sEPSCs (Fig. 4B,D). Strikingly, a single treatment with ISRIB ~one month after rTBI reversed this synaptic hyperexcitability, decreasing the frequency of synaptic input to sham levels (Fig. 4B,C). Excitatory synaptic frequency and amplitude did not change after rTBI or with ISRIB treatment in type B neurons (Fig. 5).

## Discussion

An estimated three million TBIs are reported annually in the United States. Of the reported cases, 70-90% are considered mild<sup>44</sup> and in anywhere from 10-40% of these individuals, long-term behavioral and cognitive impairments will develop.<sup>45-47</sup>

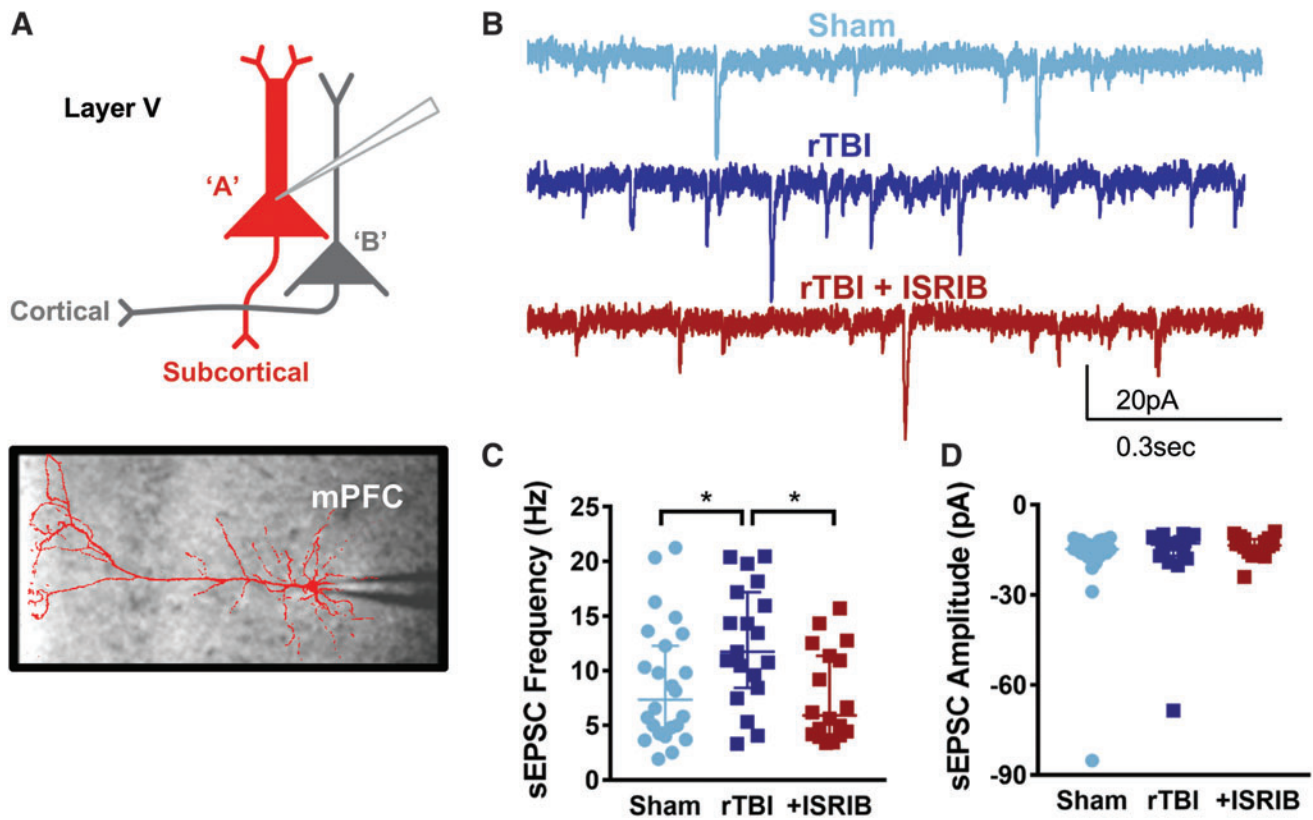


**FIG. 4.** Cell-specific vulnerability to mild repetitive traumatic brain injury (rTBI) is observed in the prefrontal cortex with an increase in the frequency of synaptic input in type A layer V pyramidal neurons that is restored after integrated stress response inhibitor (ISRIB) treatment. **(A)** Depiction of layer V pyramidal neurons indicating type A being recorded along with representative image of a filled type A pyramidal neuron overlaying image of patch pipette in the medial prefrontal cortex (mPFC). **(B)** Representative whole cell voltage-clamp recordings showing spontaneous excitatory post-synaptic currents (sEPSC) from layer V type A pyramidal neurons from sham mice (light blue), rTBI mice (dark blue), and rTBI mice treated with ISRIB (red). **(C)** The sEPSC frequency is increased in the rTBI neurons compared with both sham and rTBI+ISRIB groups ( $p=0.028$  for group effect; Kruskal-Wallis test,  $*p<0.05$  for *post hoc* tests controlling for false discovery rate). **(D)** The sEPSC amplitude is not significantly different between groups ( $p=0.469$  for group effect; Kruskal-Wallis test). The median frequency or amplitude for each neuron is represented with a symbol; solid lines indicate the median  $\pm 95\%$  confidence interval ( $n=24, 19, 18$  sham, rTBI, rTBI+ISRIB neurons, respectively, from 11 (sham), 7 (rTBI), and 9 (rTBI+ISRIB) animals/group with 1–4 neurons recorded per animal). Color image is available online.

Often deficits may not initially be observed after a single TBI; however, additional head injuries can have cumulating effects including both increased susceptibility to future injury as well as behavioral and cognitive deficits.<sup>6–8</sup> There are no clinically available therapeutics to treat or even ameliorate the devastating effects of mild rTBI. In this study, we found that male mice that received a mild TBI daily for five days (five total) displayed increased risk-taking behavior measured one and three months later. This behavior was specific to both type of trauma and sex of the animal. We detected no increase in risk-taking behavior in male mice exposed to other trauma models including a single focal injury and a single concussive injury without rotational acceleration. Further, female mice exposed to an identical rTBI paradigm did not display increased risk-taking behavior. This persistent behavioral phenotype corroborates the long-term maladaptive behavioral effects of rTBI also observed in humans. At the cellular and functional level, we found that the risk-taking behavior was associated with increased activation of the ISR and cell-specific synaptic alterations in the type A subtype of layer V pyramidal neurons of the mPFC. Importantly, targeting the ISR using the small molecule inhibitor ISRIB reversed rTBI-induced risk-taking behavior and the associated cell-specific deficits in synaptic function. Thus, we have

identified for the first time the effectivity of ISRIB in reversing chronic behavioral deficits after rTBI along with cell-specific synaptic dysfunction in the mPFC.

In the general population, men are 40% more likely to have a TBI.<sup>48,49</sup> Studies of female athletes, however, have found that women have more concussions than men when playing the same sport,<sup>50</sup> making understanding of sex-dimorphic injury responses critical for a comprehensive appreciation of rTBI pathology. Further, a recent review suggested that in  $\sim 93\%$  of pre-clinical TBI studies, biological sex as a variable was ignored.<sup>51</sup> Here we identified a different behavioral response to rTBI (five midline impacts) in male and female mice. Whereas multiple mild traumas resulted in significant increased risk-taking behavior in male mice, this maladaptive behavioral response did not develop in female rodents. To our knowledge, this is the first study to investigate sex-dimorphic responses at a chronic time point after repetitive TBI. Only one other group has investigated sex differences acutely after a unilateral rTBI (three total impacts)—in adolescent rats and measured increased anxiety-like behavior in both male and female rats.<sup>52,53</sup> The behavioral end-point, number of impacts, or placement of the impact could account for the differences in our readouts. Other studies of repetitive head injury replicated this increase

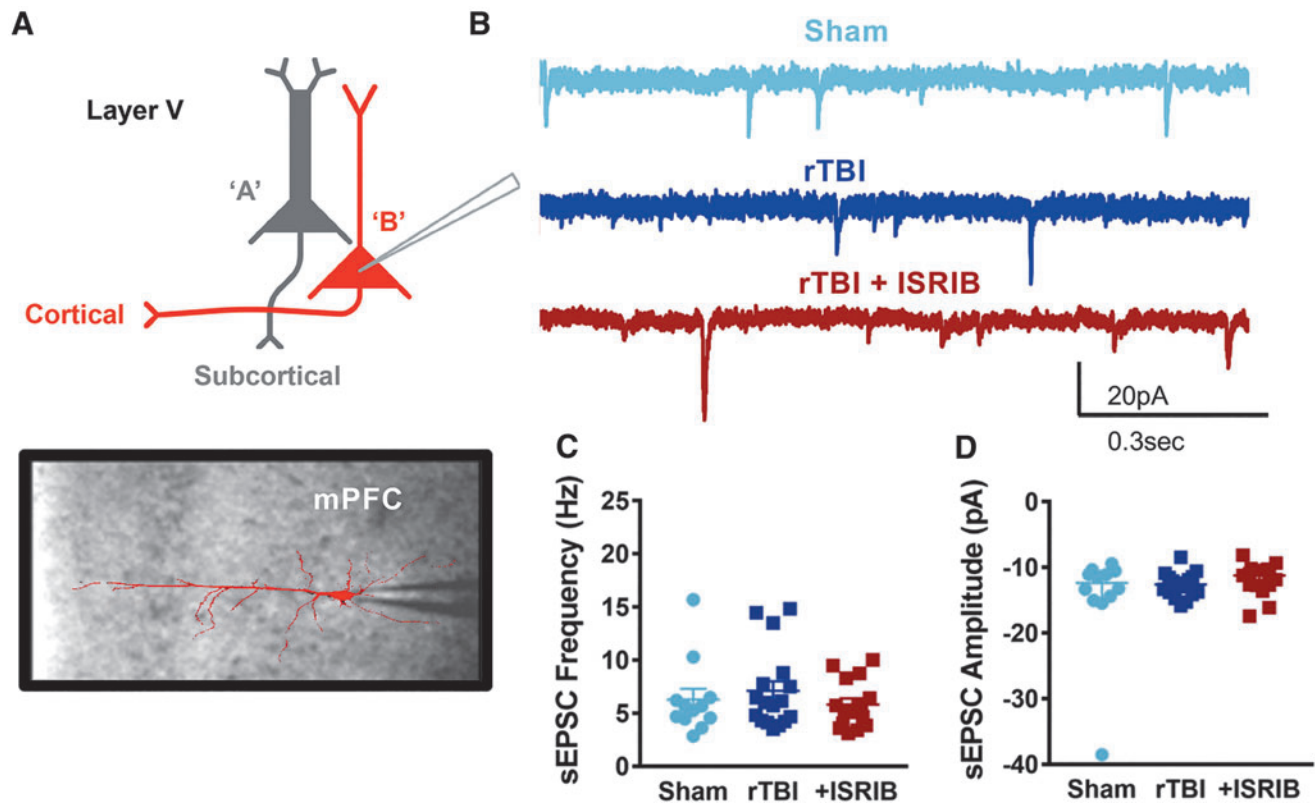


**FIG. 5.** Synaptic input in type B layer V pyramidal neurons in the prefrontal cortex is not affected by mild repetitive traumatic brain injury (rTBI) or integrated stress response inhibitor (ISRIB) treatment. (A) Depiction of layer V pyramidal neurons indicating type B being recorded along with representative image of a filled type B pyramidal neuron overlaying image of patch pipette in the medial prefrontal cortex (mPFC). (B) Representative whole cell voltage-clamp recordings showing spontaneous excitatory post-synaptic currents (sEPSC) from layer V type B pyramidal neurons from sham mice (light blue), rTBI mice (dark blue), and rTBI mice treated with ISRIB (red). (C) The sEPSC frequency is not significantly different between groups ( $p=0.664$  for group effect; Kruskal-Wallis test). (D) The sEPSC amplitude is not significantly different between groups ( $p=0.401$  for group effect; Kruskal-Wallis test). The median frequency or amplitude for each neuron is represented with a symbol; solid lines indicate the median  $\pm 95\%$  confidence interval ( $n=12, 17, 15$  sham, rTBI, rTBI+ISRIB neurons, respectively, from 7 (sham), 5 (rTBI), and 8 (rTBI+ISRIB) animals/group with 1–4 neurons recorded per animal). Color image is available online.

in risk-taking phenotype in male mice<sup>54–57</sup>; however, sex differences were not evaluated in these previous reports.

Young female athletes are reported to have increased rates of concussion and more neurological symptoms that last longer compared with male counterparts.<sup>58,59</sup> The frequency of global disability measured in females after work-related concussion, however, was lower when compared with male cohorts.<sup>58</sup> Importantly, superior executive function measured with the Wisconsin Card Sorting Test was identified in females compared with males with TBI after controlling for education, ethnicity, and injury severity.<sup>61</sup> These studies suggest that much more research is needed to identify factors affecting vulnerability or resilience to TBI, especially rTBI, in women.

Likewise, the physiology underlying the sex-dimorphic response to rTBI that we have identified here is unclear. The biophysics of injury to the mPFC might be different in female mice given their smaller head size.<sup>62</sup> Notably, the volume of the mPFC exhibits sexual dimorphism in humans<sup>63</sup> and inhibitory neuronal subtypes show striking differences in composition by sex in some brain regions.<sup>64</sup> These differences might contribute to increased vulnerability to repetitive brain injury in male mice; however, the exact mechanism remains to be determined.

The ISR is a universal pathway that responds to a wide array of cellular stressors. The central regulatory step of the ISR is the

phosphorylation of the  $\alpha$ -subunit of eIF2.<sup>18,65–67</sup> Phosphorylation of eIF2 $\alpha$  leads to inhibition of general protein synthesis,<sup>22,23</sup> with translation of a few select proteins including ATF4<sup>28,29</sup> and BACE-1.<sup>24–27</sup> Previously, our group and others have identified that both focal and diffuse head injuries induce phosphorylation of eIF2 $\alpha$  in the brain chronically after injury.<sup>19–21</sup> Brief interference with this pathway using the small-molecule inhibitor ISRIB at chronic time points completely rescued trauma-induced hippocampal-dependent learning and memory deficits.<sup>19</sup> In this study, we demonstrated that rTBI results in chronic activation of the ISR, and ISRIB administration at  $\sim$ one month post-injury significantly reduced ATF4 and BACE-1 protein levels to those comparable to sham. Further, ISRIB treatment completely reversed rTBI-induced risk-taking behavior, and this rescue was long-lasting. Interestingly, while ISRIB treatment had no effect in sham animals acutely after treatment, we measured a long-term effect in the elevated plus maze assay at the three month time point, similar to our previous reports that ISRIB treatment can improve performance in naïve and sham rodents.<sup>19,33–35</sup> Our previous studies have focused on hippocampal-dependent memory, but risk-taking behavior has been associated with PFC function.<sup>43,68</sup> Taken together, these studies suggest that ISR intervention strategies can restore and modify not only



cognitive, but also behavioral changes controlled by diverse brain regions.

The mPFC integrates complex sensory information and modulates behavioral response<sup>69</sup>; as such, deficits in mPFC function have been linked to cognitive and behavioral dysfunction, including risk-taking behavior.<sup>43,68</sup> Here, we demonstrated that an increase in the frequency of excitatory synaptic input specifically occurs in the type A layer V pyramidal neuron subtype at chronic time points after mild rTBI, associated with risk-taking behavior. This is the first study to examine mPFC function after rTBI, and only one other study has evaluated synaptic input in the mPFC after a single moderate TBI. Smith and associates<sup>70</sup> identified a prominent increase in the frequency of spontaneous and miniature excitatory post-synaptic currents and a decrease in the amplitude of inhibitory input in layer 2/3 pyramidal neurons ~one week after a single lateral fluid percussion injury that was associated with deficits in working memory. In contrast, layer V neurons did not show changes in synaptic input, and risk-taking behavior was not evaluated. The discrepancy between our studies could be because of several factors, including a different (and not repetitive) model of injury, the more subacute rather than chronic timing of their studies, and/or in particular, the fact that they did not specifically evaluate layer V neuronal subtypes.

Subtype-specific vulnerability of type A or subcortically projecting L5 pyramidal neurons has been identified in other animal models with behavioral deficits, including models of autism,<sup>71</sup> suggesting that changes in synaptic input to these neurons might also directly affect mPFC-mediated behaviors after TBI. Properties of synaptic input to type A neurons in the mPFC have been hypothesized to be specifically responsive to focal strong input in the dendritic tree, ultimately providing a salient signal to subcortical structures.<sup>41</sup> Thus, altered synaptic properties in type A neurons after repetitive injury might be responsible for lack of appreciation of danger or risk in the animal.

Not only did we identify subtype-specific vulnerability in layer V after TBI, we notably found that this synaptic hyperexcitability could be rescued by a single injection of ISRIB at one month after injury. ISRIB has been found to exert activity-dependent changes in synaptic function including blocking metabotropic glutamate receptor-mediated long-term depression in the ventral tegmental area (VTA) *in vitro*<sup>72</sup> and enhancing cocaine-induced long-term potentiation in the VTA after *in vivo* injection.<sup>73</sup> In addition, ISRIB application *in vitro* has rescued TBI-induced deficits in LTP in the hippocampus.<sup>19</sup> Here, we expand the range of ISRIB treatment effects to include not only activity-dependent synaptic regulation, but also a rescue of cell-specific vulnerability in synaptic hyperexcitability. These intriguing findings suggest that cell-specific vulnerability, a common feature in neurodegenerative disease and now identified in rTBI, might be specifically addressed with inhibiting cellular stress.

## Conclusion

We demonstrated that rTBI leads to a sex-dependent increase in long-lasting risk-taking behavior in male mice associated with synaptic hyperexcitability specifically in type A L5 pyramidal neurons of the mPFC. For the first time, we identified that inhibition of the integrated stress response with ISRIB rescues a mPFC-dependent behavioral deficit and the associated cell-specific vulnerability. Overall, these results suggest that the ISR pathway may represent a key target in maladaptive circuit and cognitive functions after injury.

## Acknowledgments

This work was supported by National Institutes of Health NIA grants R01AG056770 (SR), the generous support of the Roger's family to SR and PW, the Weill Innovation Award to SR and PW, Calico Life Sciences to PW, and "Programa de Apoyo a Centros con Financiamiento Basal AFB 170004" to SB at Fundacion Ciencia & Vida. PW is an Investigator of the Howard Hughes Medical Institute. KK was supported by an NRSA post-doctoral fellowship from the NIA F32AG054126. EF is supported by the National Institute for General Medicine (NIGMS) Initiative for Maximizing Student Development (R25GM056847) and the National Science Foundation (NSF) Graduate Fellowship Program. AN is supported by the National Center for Advanced Translational Sciences at NIH (UCSF-CTSI Grant Number TL1 TR001871) and the NIH/NINDS (K08NS114170).

## Author Disclosure Statement

P.W. is an inventor on U.S. Patent 9708247 held by the Regents of the University of California that describes ISRIB and its analogs. Rights to the invention have been licensed by UCSF to Calico. For the remaining authors, no competing financial interests exist.

## Supplementary Material

Supplementary Figure S1  
 Supplementary Figure S2  
 Supplementary Figure S3  
 Supplementary Table S1  
 Supplementary Table S2  
 Supplementary Table S3  
 Supplementary Table S4  
 Supplementary Table S5  
 Supplementary Table S6

## References

- Smith, D.H., Johnson, V.E., and Stewart, W. (2013). Chronic neuropathologies of single and repetitive TBI: substrates of dementia? *Nat. Rev. Neurol.* 9, 211–221.
- DeKosky, S.T., Ikonovic, M.D., and Gandy, S. (2010). Traumatic brain injury—football, warfare, and long-term effects. *N. Engl. J. Med.* 363, 1293–1296.
- Engberg, A.W., and Teasdale, T.W. (2004). Psychosocial outcome following traumatic brain injury in adults: a long-term population-based follow-up. *Brain Inj.* 18, 533–545.
- Sullivan, P., Petitti, D., and Barbaccia, J. (1987). Head trauma and age of onset of dementia of the Alzheimer type. *JAMA* 257, 2289–2290.
- Nelson, L.D., Temkin, N.R., Dikmen, S., Barber, J., Giacino, J.T., Yuh, E., Levin, H.S., McCrea, M.A., Stein, M.B., Mukherjee, P., Okonkwo, D.O., Diaz-Arrastia, R., Manley, G.T., and the TRACK-TBI Investigators, Adeoye, O., Badjatia, N., Boase, K., Bodien, Y., Bullock, M.R., Chesnut, R., Corrigan, J.D., Crawford, K., MIS, Duhaime, A.C., Ellenbogen, R., Feeser, V.R., Ferguson, A., Foreman, B., Gardner, R., Gaudette, E., Gonzalez, L., Gopinath, S., Gullapalli, R., Hemphill, J.C., Hotz, G., Jain, S., Korley, F., Kramer, J., Kreitzer, N., Lindsell, C., Machamer, J., Madden, C., Martin, A., McAllister, T., Merchant, R., Noel, F., Palacios, E., Perl, D., Puccio, A., Rabinowitz, M., Robertson, C.S., Rosand, J., Sander, A., Satris, G., Schnyer, D., Seabury, S., Sherer, M., Taylor, S., Toga, A., Valadka, A., Vassar, M.J., Vespa, P., Wang, K., Yue, J.K., and Zafonte, R. (2019). Recovery after mild traumatic brain injury in patients presenting to US Level I trauma centers: a transforming research and clinical knowledge in traumatic brain injury (TRACK-TBI) study. *JAMA Neurol.* E-pub ahead of print.
- Lasry, O., Liu, E.Y., Powell, G.A., Ruel-Laliberte, J., Marcoux, J., and Buckeridge, D.L. (2017). Epidemiology of recurrent traumatic brain

- injury in the general population: a systematic review. *Neurology* 89, 2198–2209.
7. Belanger, H.G., Spiegel, E., and Vanderploeg, R.D. (2010). Neuropsychological performance following a history of multiple self-reported concussions: a meta-analysis. *J. Int. Neuropsychol. Soc.* 16, 262–267.
  8. Geddes, J.F., Vowles, G.H., Nicoll, J.A., and Revesz, T. (1999). Neuronal cytoskeletal changes are an early consequence of repetitive head injury. *Acta Neuropathol.* 98, 171–178.
  9. Manley, G., Gardner, A.J., Schneider, K.J., Guskiewicz, K.M., Bailes, J., Cantu, R.C., Castellani, R.J., Turner, M., Jordan, B.D., Randolph, C., Dvorak, J., Hayden, K.A., Tator, C.H., McCrory, P., and Iverson, G.L. (2017). A systematic review of potential long-term effects of sport-related concussion. *Br. J. Sports Med.* 51, 969–977.
  10. McAllister, T., and McCrea, M. (2017). Long-term cognitive and neuropsychiatric consequences of repetitive concussion and head-impact exposure. *J. Athl. Train.* 52, 309–317.
  11. Castile, L., Collins, C.L., McIlvain, N.M., and Comstock, R.D. (2012). The epidemiology of new versus recurrent sports concussions among high school athletes, 2005–2010. *Br. J. Sports Med.* 46, 603–610.
  12. McKee, A.C., Cantu, R.C., Nowinski, C.J., Hedley-Whyte, E.T., Gavett, B.E., Budson, A.E., Santini, V.E., Lee, H.S., Kubilus, C.A., and Stern, R.A. (2009). Chronic traumatic encephalopathy in athletes: progressive tauopathy after repetitive head injury. *J. Neuropathol. Exp. Neurol.* 68, 709–735.
  13. Stern, R.A., Daneshvar, D.H., Baugh, C.M., Seichepine, D.R., Montenigro, P.H., Riley, D.O., Fritts, N.G., Stamm, J.M., Robbins, C.A., McHale, L., Simkin, I., Stein, T.D., Alvarez, V.E., Goldstein, L.E., Budson, A.E., Kowall, N.W., Nowinski, C.J., Cantu, R.C., and McKee, A.C. (2013). Clinical presentation of chronic traumatic encephalopathy. *Neurology* 81, 1122–1129.
  14. Mez, J., Daneshvar, D.H., Kiernan, P.T., Abdolmohammadi, B., Alvarez, V.E., Huber, B.R., Alosco, M.L., Solomon, T.M., Nowinski, C.J., McHale, L., Cormier, K.A., Kubilus, C.A., Martin, B.M., Murphy, L., Baugh, C.M., Montenigro, P.H., Chaisson, C.E., Tripodis, Y., Kowall, N.W., Weuve, J., McClean, M.D., Cantu, R.C., Goldstein, L.E., Katz, D.I., Stern, R.A., Stein, T.D., and McKee, A.C. (2017). Clinicopathological evaluation of chronic traumatic encephalopathy in players of American football. *JAMA* 318, 360–370.
  15. Juengst, S.B., Kumar, R.G., Arenth, P.M., and Wagner, A.K. (2014). Exploratory associations with tumor necrosis factor- $\alpha$ , disinhibition and suicidal endorsement after traumatic brain injury. *Brain Behav. Immun.* 41, 134–143.
  16. Polinder, S., Cnossen, M.C., Real, R.G.L., Covic, A., Gorbunova, A., Voormolen, D.C., Master, C.L., Haagsma, J.A., Diaz-Arrastia, R., and von Steinbuechel, N. (2018). A multidimensional approach to post-concussion symptoms in mild traumatic brain injury. *Front. Neurol.* 9, 1113.
  17. Tellier, A., Marshall, S.C., Wilson, K.G., Smith, A., Perugini, M., and Stiell, I.G. (2009). The heterogeneity of mild traumatic brain injury: Where do we stand? *Brain Inj.* 23, 879–887.
  18. Donnelly, N., Gorman, A.M., Gupta, S., and Samali, A. (2013). The eIF2 $\alpha$  kinases: their structures and functions. *Cell Mol. Life Sci.* 70, 3493–3511.
  19. Chou, A., Krukowski, K., Jopson, T., Zhu, P.J., Costa-Mattioli, M., Walter, P., and Rosi, S. (2017). Inhibition of the integrated stress response reverses cognitive deficits after traumatic brain injury. *Proc. Natl. Acad. Sci. U. S. A.* 114, E6420–E6426.
  20. Dash, P.K., Hylin, M.J., Hood, K.N., Orsi, S.A., Zhao, J., Redell, J.B., Tsvetkov, A.S., and Moore, A.N. (2015). Inhibition of eukaryotic initiation factor 2  $\alpha$  phosphatase reduces tissue damage and improves learning and memory after experimental traumatic brain injury. *J. Neurotrauma* 32, 1608–1620.
  21. Rubovitch, V., Barak, S., Rachmany, L., Goldstein, R.B., Zilberstein, Y., and Pick, C.G. (2015). The neuroprotective effect of salubrinal in a mouse model of traumatic brain injury. *Neuromolecular Med.* 17, 58–70.
  22. Hinnebusch, A.G., Ivanov, I.P., and Sonenberg, N. (2016). Translational control by 5'-untranslated regions of eukaryotic mRNAs. *Science* 352, 1413–1416.
  23. Sonenberg, N., and Hinnebusch, A.G. (2009). Regulation of translation initiation in eukaryotes: mechanisms and biological targets. *Cell* 136, 731–745.
  24. De Pietri Tonelli, D., Mihailovich, M., Di Cesare, A., Codazzi, F., Grohovaz, F., and Zacchetti, D. (2004). Translational regulation of BACE-1 expression in neuronal and non-neuronal cells. *Nucleic Acids Res.* 32, 1808–1817.
  25. Lammich, S., Schobel, S., Zimmer, A.K., Lichtenthaler, S.F., and Haass, C. (2004). Expression of the Alzheimer protease BACE1 is suppressed via its 5'-untranslated region. *EMBO Rep.* 5, 620–625.
  26. Mihailovich, M., Thermann, R., Grohovaz, F., Hentze, M.W., and Zacchetti, D. (2007). Complex translational regulation of BACE1 involves upstream AUGs and stimulatory elements within the 5' untranslated region. *Nucleic Acids Res.* 35, 2975–2985.
  27. O'Connor, T., Sadleir, K.R., Maus, E., Velliquette, R.A., Zhao, J., Cole, S.L., Eimer, W.A., Hitt, B., Bembinster, L.A., Lammich, S., Lichtenthaler, S.F., Hebert, S.S., De Strooper, B., Haass, C., Bennett, D.A., and Vassar, R. (2008). Phosphorylation of the translation initiation factor eIF2 $\alpha$  increases BACE1 levels and promotes amyloidogenesis. *Neuron* 60, 988–1009.
  28. Chen, A., Muzzio, I.A., Malleret, G., Bartsch, D., Verbitsky, M., Pavlidis, P., Yonan, A.L., Vronskaya, S., Grody, M.B., Cepeda, I., Gilliam, T.C., and Kandel, E.R. (2003). Inducible enhancement of memory storage and synaptic plasticity in transgenic mice expressing an inhibitor of ATF4 (CREB-2) and C/EBP proteins. *Neuron* 39, 655–669.
  29. Pasini, S., Corona, C., Liu, J., Greene, L.A., and Shelanski, M.L. (2015). Specific downregulation of hippocampal ATF4 reveals a necessary role in synaptic plasticity and memory. *Cell Rep.* 11, 183–191.
  30. Costa-Mattioli, M., Gobert, D., Stern, E., Gamache, K., Colina, R., Cuello, C., Sossin, W., Kaufman, R., Pelletier, J., Rosenblum, K., Krnjevic, K., Lacaille, J.C., Nader, K., and Sonenberg, N. (2007). eIF2 $\alpha$  phosphorylation bidirectionally regulates the switch from short- to long-term synaptic plasticity and memory. *Cell* 129, 195–206.
  31. Batista, G., Johnson, J.L., Dominguez, E., Costa-Mattioli, M., and Pena, J.L. (2016). Translational control of auditory imprinting and structural plasticity by eIF2 $\alpha$ . *Elife* 5.
  32. Jiang, Z., Belforte, J.E., Lu, Y., Yabe, Y., Pickel, J., Smith, C.B., Je, H.S., Lu, B., and Nakazawa, K. (2010). eIF2 $\alpha$  Phosphorylation-dependent translation in CA1 pyramidal cells impairs hippocampal memory consolidation without affecting general translation. *J. Neurosci.* 30, 2582–2594.
  33. Sidrauski, C., Acosta-Alvear, D., Khoutorsky, A., Vedantham, P., Hearn, B.R., Li, H., Gamache, K., Gallagher, C.M., Ang, K.K., Wilson, C., Okreglak, V., Ashkenazi, A., Hann, B., Nader, K., Arkin, M.R., Renslo, A.R., Sonenberg, N., and Walter, P. (2013). Pharmacological brake-release of mRNA translation enhances cognitive memory. *Elife* 2, e00498.
  34. Sidrauski, C., McGeachy, A.M., Ingolia, N.T., and Walter, P. (2015). The small molecule ISRIB reverses the effects of eIF2 $\alpha$  phosphorylation on translation and stress granule assembly. *Elife* 4.
  35. Sidrauski, C., Tsai, J.C., Kampmann, M., Hearn, B.R., Vedantham, P., Jaishankar, P., Sokabe, M., Mendez, A.S., Newton, B.W., Tang, E.L., Verschuere, E., Johnson, J.R., Krogan, N.J., Fraser, C.S., Weissman, J.S., Renslo, A.R., and Walter, P. (2015). Pharmacological dimerization and activation of the exchange factor eIF2B antagonizes the integrated stress response. *Elife* 4, e07314.
  36. Nolan, A., Hennessy, E., Krukowski, K., Guglielmetti, C., Chaumeil, M.M., Sohal, V.S., and Rosi, S. (2018). Repeated mild head injury leads to wide-ranging deficits in higher-order cognitive functions associated with the prefrontal cortex. *J. Neurotrauma* 35, 2425–2434.
  37. Krukowski, K., Chou, A., Feng, X., Tiret, B., Paladini, M.S., Riparip, L.K., Chaumeil, M.M., Lemere, C., and Rosi, S. (2018). Traumatic brain injury in aged mice induces chronic microglia activation, synapse loss, and complement-dependent memory deficits. *Int. J. Mol. Sci.* 19.
  38. Namjoshi, D.R., Cheng, W.H., McInnes, K.A., Martens, K.M., Carr, M., Wilkinson, A., Fan, J., Robert, J., Hayat, A., Crompton, P.A., and Wellington, C.L. (2014). Merging pathology with biomechanics using CHIMERA (Closed-Head Impact Model of Engineered Rotational Acceleration): a novel, surgery-free model of traumatic brain injury. *Mol. Neurodegener.* 9, 55.
  39. Namjoshi, D.R., Cheng, W.H., Bashir, A., Wilkinson, A., Stukas, S., Martens, K.M., Whyte, T., Abebe, Z.A., McInnes, K.A., Crompton, P.A., and Wellington, C.L. (2017). Defining the biomechanical and biological threshold of murine mild traumatic brain injury using CHIMERA (Closed Head Impact Model of Engineered Rotational Acceleration). *Exp. Neurol.* 292, 80–91.

40. Chou, A., Krukowski, K., Morganti, J.M., Riparip, L.K., and Rosi, S. (2018). Persistent infiltration and impaired response of peripherally-derived monocytes after traumatic brain injury in the aged brain. *Int. J. Mol. Sci.* 19.
41. Lee, A.T., Gee, S.M., Vogt, D., Patel, T., Rubenstein, J.L., and Sohal, V.S. (2014). Pyramidal neurons in prefrontal cortex receive subtype-specific forms of excitation and inhibition. *Neuron* 81, 61–68.
42. Lister, R.G. (1987). The use of a plus-maze to measure anxiety in the mouse. *Psychopharmacology (Berl)* 92, 180–185.
43. Bogg, T., Fukunaga, R., Finn, P.R., and Brown, J.W. (2012). Cognitive control links alcohol use, trait disinhibition, and reduced cognitive capacity: evidence for medial prefrontal cortex dysregulation during reward-seeking behavior. *Drug Alcohol Depend.* 122, 112–118.
44. Cassidy, J.D., Carroll, L.J., Peloso, P.M., Borg, J., von Holst, H., Holm, L., Kraus, J., Coronado, V.G., and Injury, W.H.O. Collaborating Centre Task Force on Mild Traumatic Brain Injury. (2004). Incidence, risk factors and prevention of mild traumatic brain injury: results of the WHO Collaborating Centre Task Force on Mild Traumatic Brain Injury. *J. Rehabil. Med. Suppl* 43, 28–60.
45. Binder, L.M., Rohling, M.L., and Larrabee, G.J. (1997). A review of mild head trauma. Part I: meta-analytic review of neuropsychological studies. *J. Clin. Exp. Neuropsychol.* 19, 421–431.
46. Willer, B., and Leddy, J.J. (2006). Management of concussion and post-concussion syndrome. *Curr. Treat. Options Neurol.* 8, 415–426.
47. Mittenberg, W., Canyock, E.M., Condit, D., and Patton, C. (2001). Treatment of post-concussion syndrome following mild head injury. *J. Clin. Exp. Neuropsychol.* 23, 829–836.
48. Faul, M., and Coronado, V. (2015). Epidemiology of traumatic brain injury. *Handb. Clin. Neurol.* 127, 3–13.
49. Coronado, V.G., McGuire, L.C., Sarmiento, K., Bell, J., Lionbarger, M.R., Jones, C.D., Geller, A.I., Khoury, N., and Xu, L. (2012). Trends in traumatic brain injury in the U.S. and the public health response: 1995–2009. *J. Safety Res.* 43, 299–307.
50. Covassin, T., Moran, R., and Elbin, R.J. (2016). Sex differences in reported concussion injury rates and time loss from participation: an update of the National Collegiate Athletic Association Injury Surveillance Program from 2004–2005 Through 2008–2009. *J. Athl. Train.* 51, 189–194.
51. Spani, C.B., Braun, D.J., and Van Eldik, L.J. (2018). Sex-related responses after traumatic brain injury: considerations for preclinical modeling. *Front. Neuroendocrinol.* 50, 52–66.
52. Yamakawa, G.R., Lengkeek, C., Salberg, S., Spanswick, S.C., and Mychasiuk, R. (2017). Behavioral and pathophysiological outcomes associated with caffeine consumption and repetitive mild traumatic brain injury (RmTBI) in adolescent rats. *PLoS One* 12, e0187218.
53. Wright, D.K., O'Brien, T.J., Shultz, S.R., and Mychasiuk, R. (2017). Sex matters: repetitive mild traumatic brain injury in adolescent rats. *Ann. Clin. Transl. Neurol.* 4, 640–654.
54. Mouzon, B.C., Bachmeier, C., Ferro, A., Ojo, J.O., Crynen, G., Acker, C.M., Davies, P., Mullan, M., Stewart, W., and Crawford, F. (2014). Chronic neuropathological and neurobehavioral changes in a repetitive mild traumatic brain injury model. *Ann. Neurol.* 75, 241–254.
55. Petraglia, A.L., Plog, B.A., Dayawansa, S., Chen, M., Dashnaw, M.L., Czerniecka, K., Walker, C.T., Viterise, T., Hyrien, O., Iliff, J.J., Deane, R., Nedergaard, M., and Huang, J.H. (2014). The spectrum of neurobehavioral sequelae after repetitive mild traumatic brain injury: a novel mouse model of chronic traumatic encephalopathy. *J. Neurotrauma* 31, 1211–1224.
56. Kondo, A., Shahpasand, K., Mannix, R., Qiu, J., Moncaster, J., Chen, C.H., Yao, Y., Lin, Y.M., Driver, J.A., Sun, Y., Wei, S., Luo, M.L., Albayram, O., Huang, P., Rotenberg, A., Ryo, A., Goldstein, L.E., Pascual-Leone, A., McKee, A.C., Meehan, W., Zhou, X.Z., and Lu, K.P. (2015). Antibody against early driver of neurodegeneration cis P-tau blocks brain injury and tauopathy. *Nature* 523, 431–436.
57. Mouzon, B.C., Bachmeier, C., Ojo, J.O., Acker, C.M., Ferguson, S., Paris, D., Ait-Ghezala, G., Crynen, G., Davies, P., Mullan, M., Stewart, W., and Crawford, F. (2017). Lifelong behavioral and neuropathological consequences of repetitive mild traumatic brain injury. *Ann. Clin. Transl. Neurol.* 5, 64–80.
58. Mollayeva, T., El-Khechen-Richandi, G., and Colantonio, A. (2018). Sex & gender considerations in concussion research. *Concussion* 3, CNC51.
59. Covassin, T., Schatz, P., and Swanik, C.B. (2007). Sex differences in neuropsychological function and post-concussion symptoms of concussed collegiate athletes. *Neurosurgery* 61, 345–350.
60. Hatskevich, C.W., Itkis, M.L., and Maloletnev, V.I. (1992). Off-line methods for detection and correction of EEG artefacts of various origin. *Int. J. Psychophysiol.* 12, 179–185.
61. Niemeier, J.P., Marwitz, J.H., Leshner, K., Walker, W.C., and Bushnik, T. (2007). Gender differences in executive functions following traumatic brain injury. *Neuropsychol. Rehabil.* 17, 293–313.
62. Caccese, J.B., Buckley, T.A., Tierney, R.T., Arbogast, K.B., Rose, W.C., Glutting, J.J., and Kaminski, T.W. (2018). Head and neck size and neck strength predict linear and rotational acceleration during purposeful soccer heading. *Sports Biomech.* 17, 462–476.
63. Ruigrok, A.N., Salimi-Khorshidi, G., Lai, M.C., Baron-Cohen, S., Lombardo, M.V., Tait, R.J., and Suckling, J. (2014). A meta-analysis of sex differences in human brain structure. *Neurosci. Biobehav. Rev.* 39, 34–50.
64. Kim, Y., Yang, G.R., Pradhan, K., Venkataraju, K.U., Bota, M., Garcia Del Molino, L.C., Fitzgerald, G., Ram, K., He, M., Levine, J.M., Mitra, P., Huang, Z.J., Wang, X.J., and Osten, P. (2017). Brain-wide maps reveal stereotyped cell-type-based cortical architecture and subcortical sexual dimorphism. *Cell* 171, 456–469.e422.
65. Ron, D., and Harding, H.P. (2012). Protein-folding homeostasis in the endoplasmic reticulum and nutritional regulation. *Cold Spring Harb. Perspect. Biol.* 4.
66. Tsai, J.C., Miller-Vedam, L.E., Anand, A.A., Jaishankar, P., Nguyen, H.C., Renslo, A.R., Frost, A., and Walter, P. (2018). Structure of the nucleotide exchange factor eIF2B reveals mechanism of memory-enhancing molecule. *Science* 359.
67. Zyryanova, A.F., Weis, F., Faille, A., Alard, A.A., Crespillo-Casado, A., Sekine, Y., Harding, H.P., Allen, F., Parts, L., Fromont, C., Fischer, P.M., Warren, A.J., and Ron, D. (2018). Binding of ISRIB reveals a regulatory site in the nucleotide exchange factor eIF2B. *Science* 359, 1533–1536.
68. St Onge, J.R., and Floresco, S.B. (2010). Prefrontal cortical contribution to risk-based decision making. *Cereb. Cortex* 20, 1816–1828.
69. Riga, D., Matos, M.R., Glas, A., Smit, A.B., Spijker, S., and Van den Oever, M.C. (2014). Optogenetic dissection of medial prefrontal cortex circuitry. *Front. Syst. Neurosci.* 8, 230.
70. Smith, C.J., Xiong, G., Elkind, J.A., Putnam, B., and Cohen, A.S. (2015). Brain injury impairs working memory and prefrontal circuit function. *Front. Neurol.* 6, 240.
71. Brumback, A.C., Ellwood, I.T., Kjaerby, C., Iafrati, J., Robinson, S., Lee, A.T., Patel, T., Nagaraj, S., Davatolhagh, F., and Sohal, V.S. (2018). Identifying specific prefrontal neurons that contribute to autism-associated abnormalities in physiology and social behavior. *Mol. Psychiatry* 23, 2078–2089.
72. Di Prisco, G.V., Huang, W., Buffington, S.A., Hsu, C.C., Bonnen, P.E., Placzek, A.N., Sidrauski, C., Krnjevic, K., Kaufman, R.J., Walter, P., and Costa-Mattioli, M. (2014). Translational control of mGluR-dependent long-term depression and object-place learning by eIF2alpha. *Nat. Neurosci.* 17, 1073–1082.
73. Placzek, A.N., Prisco, G.V., Khatiwada, S., Sgritta, M., Huang, W., Krnjevic, K., Kaufman, R.J., Dani, J.A., Walter, P., and Costa-Mattioli, M. (2016). eIF2alpha-mediated translational control regulates the persistence of cocaine-induced LTP in midbrain dopamine neurons. *Elife* 5.

Address correspondence to:

Susanna Rosi, PhD

San Francisco General Hospital

1001 Potrero Avenue

Building#1 Room 101

San Francisco, CA 94110

USA

E-mail: susanna.rosi@ucsf.edu